Medicinal Chemistry Research (2022) 31:1771–1782
https://doi.org/10.1007/s00044-022-02943-6

MEDICINAL CHEMISTRY RESEARCH

ORIGINAL RESEARCH

Design, synthesis and molecular docking studies of novel benzimidazole-1,3,4-oxadiazole hybrids for their carbonic anhydrase inhibitory and antioxidant effects

Kaan Küçükoğlu[1] · Ulviye Acar Çevik[2] · Hayrunnisa Nadaroglu[3] · Ismail Celik[4] · Ayşen Işık[5] · Hayrani Eren Bostancı[6] · Yusuf Özkay[2] · Zafer Asım Kaplancıklı[2]

Received: 7 April 2022 / Accepted: 28 July 2022 / Published online: 8 August 2022

Abstract

In this study, eleven new compounds with a series of benzimidazole-1,3,4-oxadiazole derivatives structures were synthesized and evaluated for their human (h) carbonic anhydrase inhibitory activities against two isoforms hCA I, hCA II, and antioxidant activity. The synthesized compounds were fully characterized by spectral analysis methods such as ^{1}H-NMR, ^{13}C-NMR, and HRMS. Compared to acetazolamide ($IC_{50} = 2.26$ µM) for hCA I, the most potent compound **4a** was with the IC_{50} value of 1.322 µM and compound **4d** is the other molecule with a greater IC_{50} value ($IC_{50} = 1.989$ µM) than that of acetazolamide in these series. Among all the compounds, **4a** (1.826 µM), **4d** (1.502 µM), and **4g** (1.886 µM) are the most active hybrids against carbonic hCA II. Considering that compound **4a** containing 4-bromophenyl structure is effective on both hCA I and hCA II, it can be considered as a promising structure for the development of effective candidates with potent CA inhibitory activities. TAS assay was used to evaluate the antioxidant activities of synthesized compounds. The synthesized compound was analyzed for their in vitro cytotoxic activity on the L929 cell line by using MTT assay. In the last step of this study, molecular docking studies were performed in order to compare the biological activities of the most active molecules against the enzymes of hCAI and hCA II.

Keywords Benzimidazole · 1,3,4-Oxadiazole · Carbonic anhydrase · Molecular Docking · Antioxidant

Introduction

The benzimidazole skeleton is formed by the fusion of a benzene ring at the 4,5-positions of an imidazole ring. Since a fast proton exchange between the -NH- and =N- atoms, two tautomers can be shown for the benzimidazole molecule. Another consequence of this exchange is that this framework contains acidic and basic nitrogen atoms [1]. There is a great interest in compounds bearing benzimidazole ring due to their diverse biological activities: anti-inflammatory [2], antihelmintic [3, 4], anticancer [5], anti-protozoal [6], antihistaminic [7], proton pump inhibitory [8, 9], antiviral [10], antimalarial [11], anti-HIV [12], and anticoagulant [13].

Oxadiazole scaffold is a five-membered heterocyclic ring bearing two nitrogen atoms and one oxygen atom. There are some isomeric forms of oxadiazole: 1,2,3-oxadiazole, 1,2,4-oxadiazole, 1,2,5-oxadiazole, and 1,3,4-oxadiazole. Of these, 1,2,3-isomer is unstable because it is converted to the diazoketone tautomer [14–16]. Oxadiazole derivatives have

Supplementary information The online version contains supplementary material available at https://doi.org/10.1007/s00044-022-02943-6.

✉ Ulviye Acar Çevik
uacar@anadolu.edu.tr

[1] Department of Pharmaceutical Chemistry, Faculty of Pharmacy, Selçuk University, Konya 42130, Turkey

[2] Department of Pharmaceutical Chemistry, Faculty of Pharmacy, Anadolu University, Eskişehir 26470, Turkey

[3] Department of Food Technology, ErzurumVocational Training School, Ataturk University, 25240 Erzurum, Turkey

[4] Department of Pharmaceutical Chemistry, Faculty of Pharmacy, Erciyes University, Kayseri 38039, Turkey

[5] Department of Biochemistry, Faculty of Science, Selçuk University, Konya, Turkey

[6] Department of Biochemistry, Faculty of Pharmacy, Sivas Cumhuriyet University, Sivas, Turkey

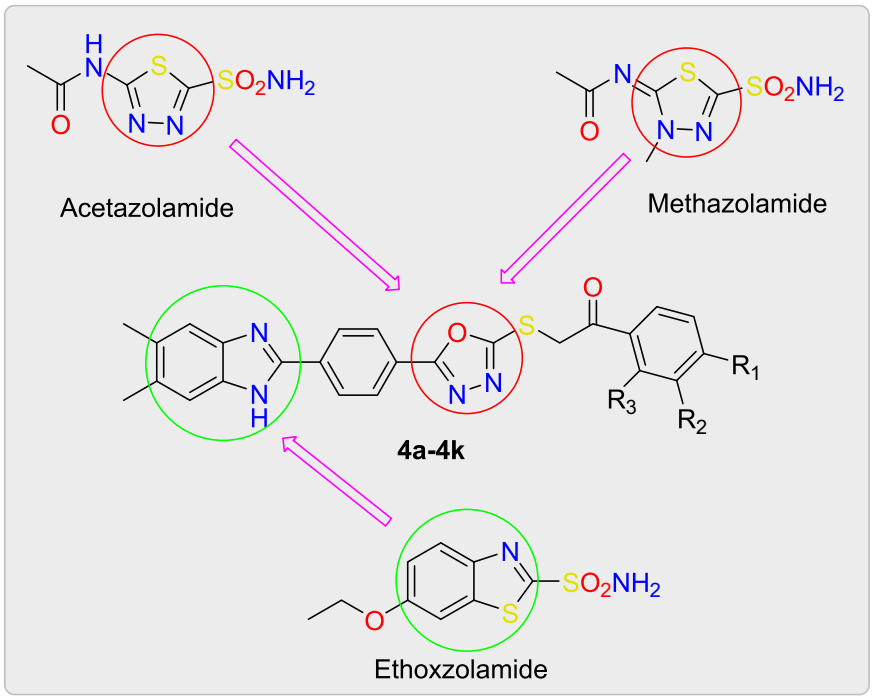

Fig. 1 General structure of acetazolamide, methazolamide and ethoxolamide and synthesized compounds

been shown to have notable biological activity and the most promising structures are compounds with 1,3,4-oxadiazole ring. It influences the physicochemical and pharmacokinetic properties of the compounds. Furthermore, 1,3,4-oxadiazole derivatives have better metabolic stability, water solubility, and lower lipophilicity than other isomeric oxadiazoles. 1,3,4-Oxadiazole ring behaves as bioisosteres of carbonyl compounds, for example, esters, amides, and carbamates. It is an essential moiety of the pharmacophore and capable of binding with the ligand. Sometimes, it is a straight aromatic linker that maintains the proper orientation of the molecule [17]. Nitrofuran derivative antibacterial furamizole, antiviral raltegravir, anti-arrhythmic nesapidil, and anticancer zibotentan are examples of commercially available drugs with 1,3,4-oxadiazole scaffold [18]. Additionally, compounds bearing 1,3,4-oxadiazole ring have been exhibited a lot of therapeutic activities such as antibacterial [19, 20], anticonvulsant [21], antitumor [22, 23], anti-tubercular [24, 25], antiviral [26], antioxidant [27], anti-inflammatory [28].

The carbonic anhydrase enzymes (CAs, EC 4.2.1.1) are a member of the zinc-containing metalloenzyme family, which alternately catalyze the conversion of carbon dioxide and water to bicarbonate and a proton [29, 30]. CAs, one of the most powerful enzymes in nature, were collected in eight different classes and sixteen isoforms [31–34]. These isoforms differentiate tissue expression patterns, functions, and kinetic properties [31, 32]. Some of them are cytosolic (CA I, CA II, CA III, CA VII, and CA XIII), some of them are membrane-bound isozymes (CA IV, CA IX, CA XII, CA XIV, and CA XV). Two of them are mitochondrial (CA VA and CA VB), and only one (CA VI) is secreted [35–38]. CAs play a pivotal role in many biochemical processes, for example, electrolyte, secretions, bone resorption, pH arrangement, calcification, respiration, lipogenesis, gluconeogenesis, and ureagenesis [36–40]. Some drugs which inhibit CA isozymes are used for the treatment of epilepsy, glaucoma, obesity, and cancer. Of these, the diuretic drugs primarily target CA II, CA IV, CA XII, and CA XIV [41, 42], while the anti-glaucoma drugs target CA II, CA IV, and CA XII [43, 44]. The target of the anti-epileptic drug is CA VII and CA XIV [45–47]. Furthermore, overexpression of hCA I isoform is connected with cerebral/retinaledema; hCA II isoform is associated with edema, glaucoma, altitude sickness and epilepsy [48, 49]. It is remarkable that ubiquitous hCA-I and II are the main off-target isoforms because these are involved in many physiological and biochemical processes. Due to the key role of this enzyme in several diseases, its inhibition is considered therapeutically important [50]. For this reason, the development of selective CA inhibitor compounds is urgently needed. Acetazolamide, methazolamide and ethoxzolamide are clinically important CA inhibitors (Fig. 1).

Numerous sulfonamides inhibit all CA isoforms nonspecifically, causing undesired side effects and reducing drug effectiveness owing to off-target inhibition. Furthermore, due to sulfa allergy, a substantial percentage of the general population cannot be treated with sulfonamides; consequently, non-sulfonamide-based CAIs must be developed. In the literature, there are many studies examining hCA activity on compounds containing benzimidazole

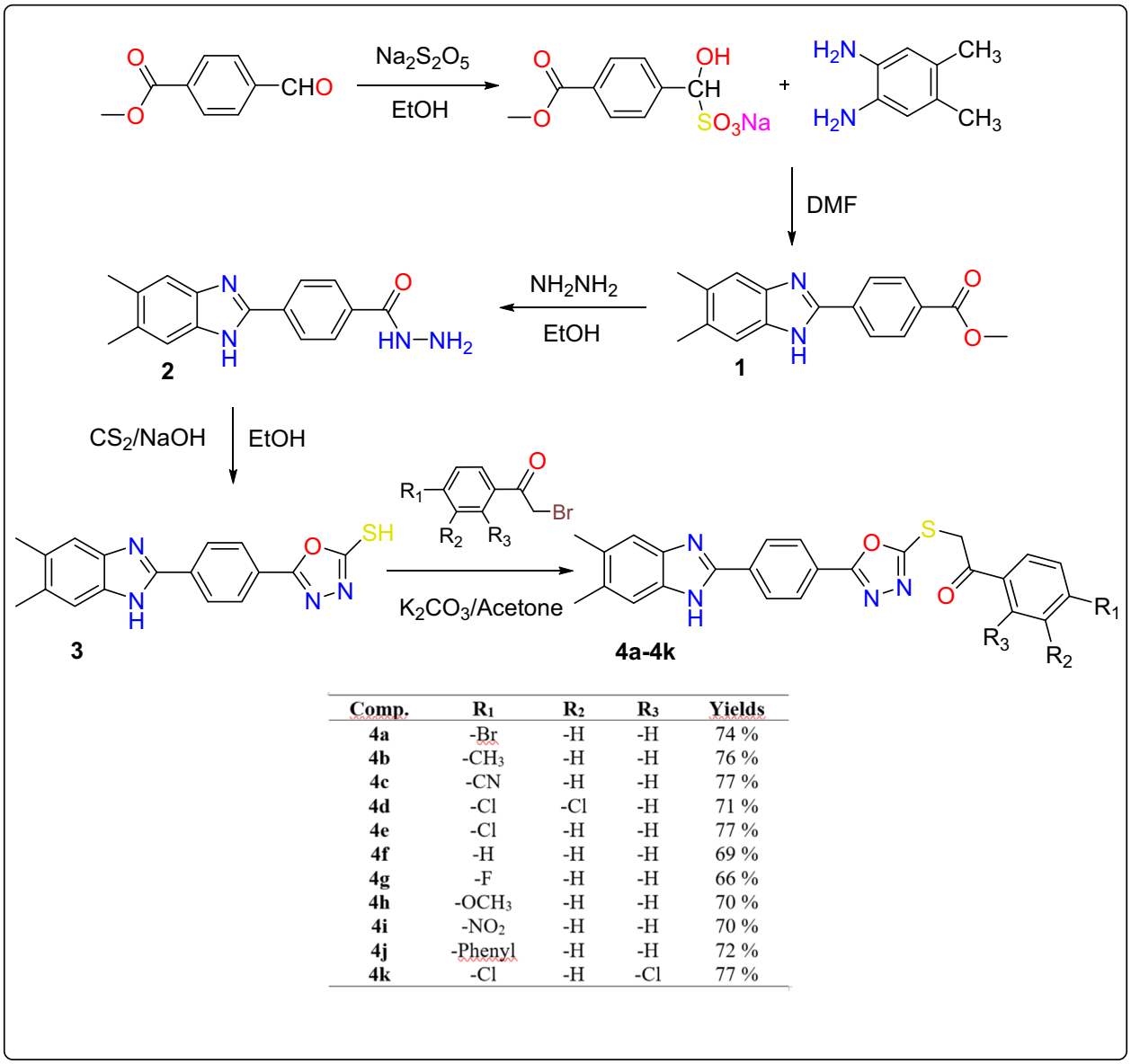

Comp.	R_1	R_2	R_3	Yields
4a	-Br	-H	-H	74 %
4b	$-CH_3$	-H	-H	76 %
4c	-CN	-H	-H	77 %
4d	-Cl	-Cl	-H	71 %
4e	-Cl	-H	-H	77 %
4f	-H	-H	-H	69 %
4g	-F	-H	-H	66 %
4h	$-OCH_3$	-H	-H	70 %
4i	$-NO_2$	-H	-H	70 %
4j	-Phenyl	-H	-H	72 %
4k	-Cl	-H	-Cl	77 %

Scheme 1 General procedure for synthesis of the final compounds **4a-4k**

structure. Therefore, in this study, benzimidazole and oxadiazole structures, which are two active structures, were combined and their effects on carbonic anhydrase enzyme were investigated [51–53].

In the current work, novel benzimidazole-1,3,4-oxadiazole hybrids bearing a benzene ring with various substituents were designed, synthesized, and investigated their inhibitory properties against hCA I and hCA II isoenzymes. The molecular docking studies of all compounds were performed on both hCA I and hCA II for protein-ligand interaction evaluations. Cytotoxicity of these synthesized compounds **4a-4k** was determined using a healthy mouse fibroblast cell line (L929). Furthermore, these compounds were also analyzed for their antioxidant capacity by TAS activity.

Results and discussion

Chemistry

The target molecules were synthesized via multiple steps as depicted in Scheme 1. The 4-(5,6-dimethyl-1*H*-benzimidazol-2-yl)benzoic acid methyl ester (1) was synthesized according to the reported literature procedure [54]. Compound **1** was treated with an excess of hydrazine hydrate in ethanol to obtain 2-(5,6-dimethylphenyl)-1*H*-benzimidazole-6-carbohydrazide derivatives (**2**). In the next step, the obtained compound **2** undergoes cyclization via a reaction with carbon disulfide and NaOH in ethanol, producing compound **3**. Finally, the reaction of compound **3** and the substituted 2-bromoacetophenone in acetone in the presence

Table 1 The IC_{50} and K_i values (μM) of the compounds **4a-4k** on hCA I and hCA II isoforms

Compound	hCA I Inhibition			hCA II Inhibition		
	IC_{50} (μM)	K_i (μM)	Type of inhibition	IC_{50} (μM)	K_i (μM)	Type of inhibition
4a	**1.322**	1.056 ± 0.07	Noncompetitive	**1.826**	1.385 ± 0.05	Noncompetitive
4b	2.812	1.375 ± 0.02	Noncompetitive	2.507	1.415 ± 0.0	Noncompetitive
4c	2.309	1.969 ± 0.021	Noncompetitive	2.283	1.692 ± 0.069	Noncompetitive
4d	**1.989**	1.544 ± 0.014	Noncompetitive	**1.502**	1.154 ± 0.022	Noncompetitive
4e	3.0999	2.435 ± 0.011	Noncompetitive	3.235	2.46 ± 0.12	Noncompetitive
4f	3.578	2.844 ± 0.017	Noncompetitive	2.612	2.60 ± 0.11	Noncompetitive
4g	2.953	2.356 ± 0.009	Noncompetitive	**1.886**	1.385 ± 0.06	Noncompetitive
4h	3.895	3.088 ± 0.018	Noncompetitive	3.649	2.769 ± 0.14	Noncompetitive
4i	2.439	1.950 ± 0.05	Noncompetitive	1.981	1.462 ± 0.006	Noncompetitive
4j	2.336	1.431 ± 0.01	Noncompetitive	2.885	1.46 ± 0.0	Noncompetitive
4k	2.333	1.427 ± 0.0	Noncompetitive	1.935	1.187 ± 0.01	Noncompetitive
Asetazolamide	2.26	1.63 ± 0.011	Noncompetitive	1.17	0.812 ± 0.01	Noncompetitive

Important results are highlighted in bold

of K_2CO_3 gave the products **4a-4k** [54].The structures of the target compounds were confirmed via ^{1}H-NMR, ^{13}C-NMR, and HRMS spectroscopy.

In vitro hCA activity

The newly synthesized benzimidazole-1,3,4-oxadiazole hybrids, **4a-4k**, were investigated to their ability two physiologically relevant hCA isozymes, hCA I and hCA II (Table 1). Commercially hCA inhibitor acetazolamide (AAZ) was used as a reference agent.

The IC_{50} values of compounds against hCA I isoform were calculated in the range of 1.322 and 3.895 μM. Compared to AAZ ($IC_{50} = 2.26$ μM), the most potent compound was **4a** with the IC_{50} value of 1.322 μM, and compound **4d** is the other molecule with a greater IC_{50} value ($IC_{50} = 1.989$ μM) than that of AAZ in compounds **4a-4k**. The activity results pointed out that no compound in these series had more effective on hCA II than AAZ ($IC_{50} = 1.17$ μM), and their IC_{50} values changed from 1.502 to 3.649 μM. Compounds **4a-4k** exhibited non-competitive inhibition on hCA I and hCA II. Obtained results indicated that the inhibitory effects of three derivatives (**4a, 4e**, and **4j**) were more significant on hCA I than hCA II, whereas **4b, 4d, 4f-4i** and **4k** showed more activity on hCA II than hCA I. The enzyme inhibitory activity of compound **4c**, which is a 4-cyano derivative, was fairly close on hCA I and hCA II isoforms and IC_{50} values of compound **4c** were 2.309 and 2.283 μM on hCA I and hCA II, respectively.

Compounds **4a-4k** showed K_i values varying from 1.056 μM to 3.088 μM on hCA I and compounds **4a, 4b, 4d, 4j**, and **4k** had lower K_i constants ranging between 1.056 μM and 1.544 μM than AAZ ($K_i = 1.63$ μM). The lowest K_i constant belonged to compound **4a** ($K_i = 1.056$ μM). The K_i constants of **4a-4k** compounds were between 1.154 μM and 2.769 μM on hCA II isozyme, and their inhibitory properties were not higher than that of AAZ ($K_i = 0.812$ μM).

Comparing compound **4d** with **4e**, the higher activity of the 4d may be possible due to the presence of chloro group at third position of phenyl ring. Compound **4g** exerted a stronger inhibition on hCA II enzyme than other compounds in the series, which is possibly due to the presence of fluoro group at para position of the phenyl ring. The presence of CH_3 or OCH_3 groups on the benzene ring of compounds **4b** and **4h** significantly reduced the activity.

Antioxidant activity

TAS

The total antioxidant capacity values greater than or equal to 1.0 mmol Trolox Equiv./L are considered as high and desired levels. Total antioxidant capacity values of the compounds between **4a-4k** were found low which is shown in Table 2. Although compounds **4e** and **4f** show partially high antioxidant capacity values, these amounts are not at the desired level.

Cytotoxicity assay

Cytotoxicity Effect of compounds **4a-4k** was evaluated against the L929 cell line. For preliminary screening, cytotoxic bioactivity of synthesized compounds was evaluated in vitro against the L929 cell line with the MTT assay. To evaluate the cytotoxic potency of target compounds, the fibroblast cells were treated with the compounds at 100 μM constant concentration. Cell viability percentages were calculated after the treatment of cells for 48 h. Preliminary

cytotoxic effect results of compounds **4a-4k** against L929 fibroblast are presented in Table 3. As a result of the maximum dose applied, all compounds except compounds **4a**, **4b**, and **4c** showed 70% and more viability. However, compounds **4b** and **4c** showed an IC_{50} value above 100 µM, but cell viability decreased to 64% and 59.5%, respectively at the maximum dose.

Molecular docking

In silico molecular docking studies are a useful method to explain the interaction between designed compounds and target proteins [55, 56]. First, self-docking was performed with acetazolamide, which is a cocrystal ligand in both hCA I (PDB ID: 3W6H) and hCA II (PDB ID: 4G0C), to validate the docking study. The RMSD for hCA I and hCA II between docked acetazolamide and natural acetazolamide were measured as 1.357 Å and 0.167 Å, respectively. After docking validation, compounds **4a-4k** were docked with hCA I and hCA II and Glide SP ligand docking with the same method, and their interaction energies were calculated. Glide gscore and emodel interaction energies of the compounds with hCA I and hCA II were given in Table 4. While the compounds gave interaction energies between −3.928 kcal/mol and −5.140 kcal/mol against hCA I, and −2.899 kcal/mol and −4.159 kcal/mol against hCA II, glide emodel energies were close to each other. The Glide docking score of the compounds in in vitro experiments showed that the interaction with hCA I was higher than with hCA II. In vitro experiments revealed the binding pose and protein-ligand interactions of compounds **4a** and **4d**, which showed the highest inhibitory activity against hCA I. As given in Fig. 2, compound **4a**; hydrophobic interactions with Leu131, Ala132, Ala134, Phe91, Leu141, Tyr204,

Table 2 mmol Trolox Equiv./L for each compound

Comp.	mmol Trolox equiv./L
4a	0.057 ± 0.013
4b	0.162 ± 0.024
4c	0.229 ± 0.042
4d	0.297 ± 0.011
4e	**0.642 ± 0.037**
4f	**0.519 ± 0.058**
4g	0.171 ± 0.038
4h	0.209 ± 0.053
4i	0.208 ± 0.072
4j	0.304 ± 0.029
4k	0.288 ± 0.081
Vitamin E	1.000 ± 0.063

Important results are highlighted in bold

Table 3 Cell Viability (%) of L929 fibroblast cell line against compounds for 48 h

Comp.	48 h Viability %
4a	37.6 ± 3.05
4b	64 ± 4.06
4c	59.5 ± 3
4d	**87.1 ± 5.13**
4e	77.6 ± 3.68
4f	75.7 ± 4.77
4g	74.8 ± 2.41
4h	71.4 ± 9.52
4i	72.7 ± 2.76
4j	72.1 ± 1.76
4k	76.9 ± 4.48
Control	100 ± 1.84

Important results are highlighted in bold

Table 4 Molecular docking interaction energies of compounds **4a-4k** with carbonic anhydrase I (hCA I) and II (hCA II)

Compounds	hCA I		hCA II	
	glide gscore	glide emodel	glide gscore	glide emodel
4a	−4.496	−44.759	−3.694	−61.462
4b	−4.613	−58.281	−3.264	−53.672
4c	−4.561	−64.284	−3.998	−60.343
4d	−4.472	−50.003	−3.554	−49.050
4e	−4.642	−42.637	−4.159	−53.893
4f	−4.764	−48.623	−3.381	−52.197
4g	−5.137	−53.895	−3.855	−49.160
4h	−3.928	−53.311	−3.342	−49.779
4i	−4.953	−61.911	−3.723	−51.241
4j	−5.140	−63.116	−2.899	−54.521
4k	−4.642	−64.725	−3.852	−54.066
Acetazolamide	−7.893	−70.685	−7.097	−67.269

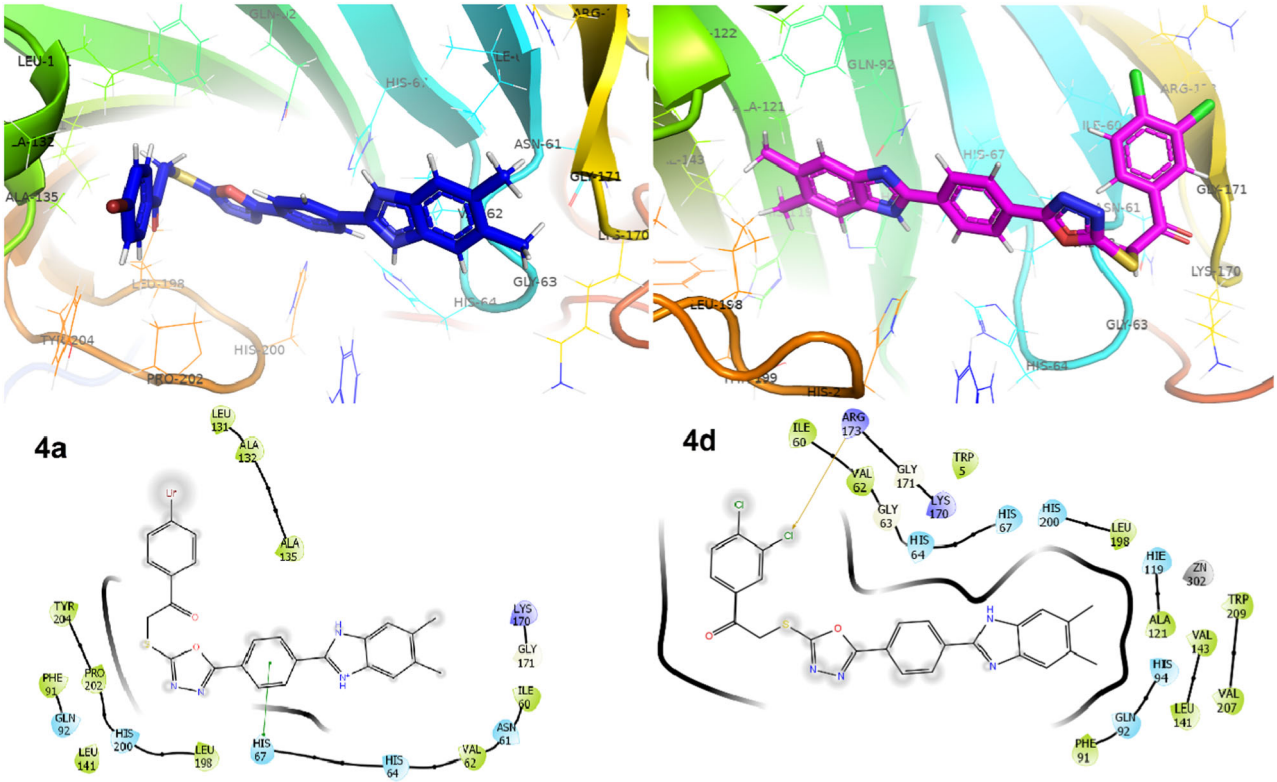

Fig. 2 Binding poses and protein-ligand interaction diagrams of most active two compounds **4a** and **4d** against human carbonic anhydrase I (PDB ID: 3W6H)

Pro202, Leu198, Val62, Ile60; polar interactions with Gln92, His200, His67, Asn61, positively charged interactions with Lys170; and Pi-Pi stacking interactions with His67. Compound **4d**; metallic interaction with Zn^{2+}; halogen bond with Arg173; hydrophobic interactions with Trp5, Ile60, Val62, Leu198, Ala121, Phe91, Leu141, Val143, Trp209, Val207; polar interactions with Gln92, His94, Hie119, His200, His67, His64; It created positively charged interactions with Arg173 and Lys170. The compounds do not interact directly with Zn^{2+} in the structure of the metalloenzymes hCA I and hCA II.

Conclusion

We have described the design, synthesis, and inhibitory properties towards carbonic anhydrase isoenzymes (hCA I and hCA II) compared to acetazolamide (AAZ). The synthesized compounds are benzimidazole-1,3,4-oxadiazole hybrid molecules and they are not sulfonamide derivatives as many compounds that show hCA inhibitory activity carries a sulfonamide group in their structure. 4-Bromo analog compound **4a** exhibited significant inhibitory activity on hCA I isoenzyme. Conversely, compounds **4a-4k** did not show more inhibitory activity than AAZ on hCA II isoenzyme. The lead compound of the series was compound **4a** in terms of IC_{50} and K_i values and this compound may be served as a model compound to design new hCA inhibitory molecules for further studies. Furthermore, the antioxidant activity evaluation in vitro of the synthesized compounds was performed by the method of TAS. As a result, the highly active compound **4e**, namely 2-((5-(4-(5,6-dimethyl-1*H*-benzimidazole-2-yl)-phenyl)-1,3,4-oxadiazole-2-yl)thio)-1-(4-chlorophenyl)-ethan-1-one was found to be the most efficient candidate among all compounds. But it is not at the desired level. Healthy mouse fibroblast cells (L929) were used to measure the cytotoxicity of the compounds. Compound **4d**, which stands out with its activity, was found to have the highest cell viability among the compounds.

Material and methods

Whole chemicals employed in the synthetic procedure were purchased from Sigma-Aldrich Chemicals (Sigma-Aldrich Corp., St. Louis, MO, USA) or Merck Chemicals (Merck KGaA, Darmstadt, Germany). Melting points of the obtained compounds were determined by the MP90 digital melting point apparatus (Mettler Toledo, OH, USA) and were uncorrected. ^{1}H-NMR and ^{13}C-NMR spectra of the

synthesized compounds were registered by a Bruker 300 MHz and 75 MHz digital FT-NMR spectrometer (Bruker Bioscience, Billerica, MA, USA) in DMSO-d_6, respectively. Splitting patterns were designated as follows: s: singlet; d: doublet; t: triplet; m: multiplet in the NMR spectra. Coupling constants (J) were reported as Hertz. M + 1 peaks were determined by Shimadzu LC/MSMS system (Shimadzu, Tokyo, Japan). All reactions were monitored by thin-layer chromatography (TLC) using Silica Gel 60 F254 TLC plates (Merck KGaA, Darmstadt, Germany).

Chemistry

Synthesis of sodium metabisulfite salt of benzaldehyde derivative

Methyl 4-formyl benzoate (5 g, 0.03 mol) was dissolved in ethanol. Sodium metabisulfite (6.84 g, 0.036 mol) in ethanol dropped dropwise into the benzaldehyde solution. After the dripping was completed, the reaction contents were stirred at room temperature for 1 h. The precipitated product was filtered off.

Synthesis of 4-(5,6-Dimethyl-1H-benzimidazol-2-yl)benzoic acid methyl ester (1)

4,5-dimethylbenzene 1,2-diamine (3 g, 0.022 mol) was dissolved in DMF, and sodium metabisulfite salt of benzaldehyde derivative (7.09 g, 0.026 mol) was added. At the end of the reaction, the product was precipitated by pouring the reaction contents into ice water. The precipitated product was filtered off and crystallized from ethanol.

Synthesis of 2-(5,6-Dimethylphenyl)-1H-benzimidazole-6-carbohydrazide derivatives (2)

Compound **2** (0.018 mol) and excess of hydrazine hydrate (5 mL) were placed in the same vial and ethanol (15 mL) was added. The mixture was refluxed for 12 h. When the reaction was completed, the mixture was poured into iced water, the product was filtered.

Synthesis of 5-[4-(5,6-Dimethyl-1H-benzimidazol)-2-yl) phenyl)-1,3,4-oxadiazole-2-thiol (3)

The hydrazide derivative compound (**2**) in ethanol was refluxed with NaOH and carbon disulfide for 5–6 h. After completion of the reaction, the solution was acidified with HCl 37%, the precipitate was filtered, washed with water, dried, and then recrystallized from ethanol.

Synthesis of 2-((5-(4-(5,6-Dimethyl-1H-benzimidazole-2-yl)-phenyl)-1,3,4-oxadiazole-2-yl)thio)-1-(substitutedphenyl)-ethan-1-one (4a-4k)

A solution of 5-[4-(5,6-dimethyl-1*H*-benzimidazol)-2-yl) phenyl)-1,3,4-oxadiazole-2-thiol (3) (0.001 mol) in acetone (10 ml), an appropriate substituted 2-bromoacetophenone derivative (0.001 mol) and potassium carbonate (0.138 g, 0.001 mol) were refluxed at 40 °C for 12 h. The solvent was evaporated, the residue was washed with water, dried, and recrystallized from ethanol.

2-((5-(4-(5,6-Dimethyl-1*H*-benzimidazole-2-yl)-phenyl)-1,3,4-oxadiazole-2-yl)thio)-1-(4-bromophenyl)-ethan-1-one (4a):

Yield: 74%. M.p. 250.3 °C. ^{1}H-NMR (300 MHz, DMSO-d_6): δ = 2.42 (6H, s, -CH_3), 5.61 (2H, s, -CH_2), 7.66 (1H, s, Aromatic C-H), 7.71–7.75 (4H, m, Aromatic C-H), 7.97–8.01 (4H, m, Aromatic C-H), 8.39–8.40 (1H, m, Aromatic CH). ^{13}C-NMR (75 MHz, DMSO-d_6): δ(ppm): 21.61, 55.07, 116.79, 119.28, 122.04, 122.61, 122.86, 126.14, 128.11, 129.51, 131.29, 131.71, 133.20, 133.99, 136.11, 140.16, 141.62, 146.09, 155.02, 157.62, 166.14. $[M + H]^+$ calcd for $C_{25}H_{19}N_4O_2SBr$: 519.0477; found: 519.0485.

2-((5-(4-(5,6-Dimethyl-1*H*-benzimidazole-2-yl)-phenyl)-1,3,4-oxadiazole-2-yl)thio)-1-(p-tolyl)-ethan-1-one (4b):

Yield: 76%. M.p. 303.2 °C. ^{1}H-NMR (300 MHz, DMSO-d_6): δ = 2.40 (9H, s, −CH_3), 5.20 (2H, s, -CH_2), 7.60–7.62 (3H, m, Aromatic C-H), 8.14–8.17 (3H, m, Aromatic C-H), 8.40–8.43 (4H, m, Aromatic C-H). ^{13}C-NMR (75 MHz, DMSO-d_6): δ(ppm): 21.24, 22.86, 57.15, 100.35, 112.97, 113.99, 115.27, 115.78, 118.12, 121.68, 126.31, 127.09, 127.96, 128.81, 130.16, 131.17, 132.87, 136.30, 139.49, 146.89, 164.33. $[M + H]^+$ calcd for $C_{26}H_{22}N_4O_2S$: 455.1520; found: 455.1536.

2-((5-(4-(5,6-Dimethyl-1*H*-benzimidazole-2-yl)-phenyl)-1,3,4-oxadiazole-2-yl)thio)-1-(4-cyanophenyl)-ethan-1-one (4c):

Yield: 77%. M.p. 308.5 °C. ^{1}H-NMR (300 MHz, DMSO-d_6): δ = 2.42 (6H, s, -CH_3), 5.27 (2H, s, -CH_2), 7.65 (2H, s, Aromatic C-H), 8.08–8.10 (2H, m, Aromatic C-H), 8.19–8.25 (2H, m, Aromatic C-H), 8.37–8.38 (2H, s, Aromatic C-H), 8.41–8.43 (2H, s, Aromatic C-H), 9.50 (1H, s, Benzimidazole -NH). ^{13}C-NMR (75 MHz, DMSO-d_6): δ(ppm): 21.31, 55.75, 113.29, 115.15, 124.22, 126.25, 127.32, 128.68, 130.24, 130.86, 132.77, 133.50, 134.85, 136.61, 139.05, 140.19, 152.25, 156.66, 162.04. $[M + H]^+$ calcd for $C_{26}H_{19}N_5O_2S$: 466.1322; found: 466.1332.

2-((5-(4-(5,6-Dimethyl-1*H*-benzimidazole-2-yl)-phenyl)-1,3,4-oxadiazole-2-yl)thio)-1-(3,4-dichlorophenyl)-ethan-1-one (4d):

Yield: 71%. M.p. 307.9 °C. ^{1}H-NMR (300 MHz, DMSO-d_6): δ = 2.41 (6H, s, -CH_3), 5.23 (2H, s, -CH_2), 7.65 (3H, s, Aromatic C-H), 8.17–8.20 (1H, m, Aromatic C-H), 8.34–8.37 (3H, m, Aromatic C-H), 8.42–8.47 (2H, m, Aroamtic C-H). ^{13}C-NMR (75 MHz, DMSO-d_6): δ(ppm): 21.23, 56.52, 113.03, 113.53, 114.30, 115.20, 115.38, 119.19, 120.30, 125.34, 127.11, 128.15, 129.42, 130.27, 130.74, 130.83, 136.66, 137.27, 146.85, 154.07, 157.22, 161.42. $[M + H]^+$ calcd for $C_{25}H_{18}N_4O_2SCl_2$: 509.0605; found: 509.0600.

2-((5-(4-(5,6-Dimethyl-1*H*-benzimidazole-2-yl)-phenyl)-1,3,4-oxadiazole-2-yl)thio)-1-(4-chlorophenyl)-ethan-1-one (4e):

Yield: 77 %. M.p. 301.4 °C. ^{1}H-NMR (300 MHz, DMSO-d_6): δ = 2.43 (6H, -CH_3), 5.24 (2H, s, -CH_2), 7.65–7.66 (3H, m, Aromatic C-H), 7.68–7.71 (1H, m, Aromatic C-H), 8.11 (1H, d, J = 8.64 Hz, Aromatic CH), 8.23 (1H, d, J = 8.55 Hz, Aromatic CH), 8.30 (1H, d, J = 8.73 Hz, Aromatic CH), 8.40–8.42 (3H, m, Aromatic CH). ^{13}C-NMR (75 MHz, DMSO-d6): δ(ppm): 21.09, 55.90, 107.85, 109.51, 113.67, 115.23, 116.14, 118.28, 120.01, 122.81, 124.03, 125.93, 127.71, 128.42, 131.23, 136.74, 139.96, 142.14, 146.40, 165.62. $[M + H]^+$ calcd for $C_{25}H_{19}N_4O_2SCl$: 475.1002; found: 475.0990.

2-((5-(4-(5,6-Dimethyl-1*H*-benzimidazole-2-yl)-phenyl)-1,3,4-oxadiazole-2-yl)thio)-1-(phenyl)-ethan-1-one (4f):

Yield: 69%. M.p. 313.7 °C. ^{1}H-NMR (300 MHz, DMSO-d6): δ = 2.41 (6H, s, -CH_3), 5.25 (2H, s, -CH_2), 7.63–7.65 (3H, m, Aromatic C-H), 8.18 (2H, d, J = 8.13 Hz, Aromatic C-H), 8.34 (1H, s, Aromatic C-H), 8.37 (2H, m, Aromatic C-H), 8.41–8.43 (2H, m, Aromatic C-H), 8.46 (1H, s, Aromatic C-H), 9.50 (1H, s, Benzimidazole -NH). ^{13}C-NMR (75 MHz, DMSO-d_6): δ(ppm): 20.43, 54.03, 114.07, 114.93, 126.25, 126.64, 127.04, 127.52, 128.19, 129.05, 129.17, 130.90, 134.51, 136.53, 138.60, 139.36, 146.68, 146.81, 155.61, 163.26. [M + H] + calcd for $C_{25}H_{20}N_4O_2S$: 441.1394; found: 441.1380.

2-((5-(4-(5,6-Dimethyl-1*H*-benzimidazole-2-yl)-phenyl)-1,3,4-oxadiazole-2-yl)thio)-1-(4-fluorophenyl)-ethan-1-one (4g):

Yield: 66%. M.p. 320.3 °C. ^{1}H-NMR (300 MHz, DMSO-d_6): δ = 2.41 (6H, s, -CH_3), 5.24 (2H, s, -CH_2), 7.62–7.64 (2H, m, Aromatic C-H), 8.17 (2H, d, J = 8.28 Hz, Aromatic C-H), 8.32–8.37 (3H, m, Aromatic C-H), 8.41 (2H, d, J = 7.53 Hz, Aromatic C-H), 8.45 (1H, s, Aromatic C-H). ^{13}C-NMR (75 MHz, DMSO-d_6): δ(ppm): 21.27, 52.96, 112.90, 115.09, 115.26, 126.23, 126.39, 126.95, 127.22, 127.69, 127.90, 128.52, 129.21, 130.11, 130.67, 130.76, 136.65, 144.68, 146.39, 162.17. $[M + H]^+$ calcd for $C_{25}H_{19}N_4O_2FS$: 459.1278; found: 459.1286.

2-((5-(4-(5,6-Dimethyl-1*H*-benzimidazole-2-yl)-phenyl)-1,3,4-oxadiazole-2-yl)thio)-1-(4-methoxyphenyl)-ethan-1-one (4h):

Yield: 70%. M.p. 313.2 °C. ^{1}H-NMR (300 MHz, DMSO-d_6): δ = 2.40 (6H, s, -CH_3), 3.87 (3H, s, -OCH_3), 5.18 (2H, s, -CH_2-), 7.60–7.61 (4H, m, Aromatic C-H), 8.15 (2H, d, J = 8.58 Hz, Aromatic C-H), 8.31-8.44 (4H, m, Aromatic C-H). ^{13}C-NMR (75 MHz, DMSO-d_6): δ(ppm): 21.24, 55.90, 57.67, 113.10, 114.48, 115.22, 118.46, 120.02, 121.88, 126.33, 127.14, 127.82, 127.99, 128.50, 130.03, 130.43, 131.45, 131.55, 136.17, 146.81, 168.42. $[M + H]^+$ calcd for $C_{26}H_{22}N_4O_3S$: 471.1491; found: 471.1485.

2-((5-(4-(5,6-Dimethyl-1*H*-benzimidazole-2-yl)-phenyl)-1,3,4-oxadiazole-2-yl)thio)-1-(4-nitrophenyl)-ethan-1-one (4i):

Yield: 70%. M.p. 308.9 °C. ^{1}H-NMR (300 MHz, DMSO-d_6): δ = 2.40 (6H, s, -CH_3), 5.31 (2H, s, -CH_2), 7.60 (2H, s, Aromatic C-H), 8.16–8.17 (4H, m, Aromatic C-H), 8.36–8.39 (4H, m, Aromatic C-H). ^{13}C-NMR (75 MHz, DMSO-d_6): δ(ppm): 21.24, 54.28, 112.99, 113.22, 115.16, 115.30, 126.14, 126.32, 126.92, 127.53, 127.90, 128.62, 130.11, 131.09, 131.19, 132.73, 134.75, 136.43, 146.77, 164.80. $M + H]^+$ calcd for $C_{25}H_{19}N_5O_4S$: 486.1285; found: 486.1231.

2-((5-(4-(5,6-Dimethyl-1*H*-benzimidazole-2-yl)-phenyl)-1,3,4-oxadiazole-2-yl)thio)-1,1'-biphenyl-ethan-1-one (4j):

Yield: 72%. M.p. 311.5 °C. ^{1}H-NMR (300 MHz, DMSO-d_6): δ = 2.41 (6H, s, -CH_3), 5.27 (2H, s, -CH_2), 7.62 (3H, s, Aromatic C-H), 7.75–7.78 (3H, m, Aromatic CH), 7.94–7.97 (3H, m, Aromatic CH), 8.18–8.21 (3H, m, Aromatic CH), 8.36–8.38 (3H, m, Aromatic CH). ^{13}C-NMR (75 MHz, DMSO-d_6): δ(ppm): 21.31, 57.35, 108.55, 113.25, 114.50, 115.44, 117.49, 119.28, 121.25, 126.45, 127.90, 128.69, 130.09, 131.40, 136.30, 136.53, 139.29, 140.15, 143.83, 146.92, 148.68, 168.63, 169.26, 178.40. $[M + H]^+$ calcd for $C_{31}H_{24}N_4O_2S$: 517.1690; found: 517.1693.

2-((5-(4-(5,6-Dimethyl-1*H*-benzimidazole-2-yl)-phenyl)-1,3,4-oxadiazole-2-yl)thio)-1-(2,4-dichlorophenyl)-ethan-1-one (4k):

Yield: 77%. M.p. 312.9 °C. ^{1}H-NMR (300 MHz, DMSO-d_6): δ = 2.42 (6H, s, -CH_3), 5.25 (2H, s, -CH_2), 7.66 (3H, s, Aromatic C-H), 8.17-8.22 (1H, m, Aromatic C-H), 8.35–8.43 (5H, m, Aromatic C-H). ^{13}C-NMR (75 MHz, DMSO-d_6): δ(ppm): 21.26, 55.38, 113.27, 114.39, 115.22, 118.33, 120.54, 122.67, 123.75, 126.23, 127.15, 128.16, 129.05, 129.48, 130.36, 130.76, 132.69, 136.71, 139.22, 146.88, 152.57, 157.24. [M + H] + calcd for $C_{25}H_{18}N_4O_2SCl_2$: 509.0612; found: 509.0600.

hCA inhibition assay

Purification of hCA I and hCA II by affinity chromatography

Fresh human blood was obtained from the blood center, Ataturk University. The blood samples were centrifuged to separate erythrocytes at 2500 rpm for 15 min and plasma and buffy coat were removed carefully. 0.9% NaCl solution was used to wash underlying erythrocytes and upper portions were also discarded. The erythrocytes were hemolyzed with distilled water at 0 °C, following it was stirred for half an hour at 4 °C. The hemolysate was centrifuged at 20000 rpm for 30 min. Then, cell membranes were separated. pH was adjusted to 8.8 by using solid Tris. The hemolysate was recovered to be applied to the column [57, 58].

The affinity gel was prepared on Sepharose-4B matrix. Sepharose-4B was activated with CNBr, L-tyrosine was covalently fitted. Sulfanilamide was coupled to tyrosine with diazotization reaction as a ligand. The hemolysate was applied to the prepared Sepharose-4B-L-tyrosine-sulfanilamide affinity column equilibrated with 25 mM Tris-HCl/0.1 M Na_2SO_4 (pH 8.7). The affinity gel was washed by using of 25 mM Tris-HCl/22 mM Na_2SO_4 (pH 8.7). The human CA isozymes (hCA I and hCA II) were eluted with 1 M NaCl/25 mM Na_2HPO_4 (pH 6.3) and 0.1 M CH_3COONa/0.5 M $NaClO_4$ (pH 5.6), respectively. All procedures were carried out at 4 °C [59].

Hydratase activity

CA activity was stated using the Wilbur-Anderson Method which was modified by Rickli et al. [59, 60]. This method, as a result hydration of CO_2 is released H^+ ions and the pH changes were determined by means of bromothymol blue indicator, based on the measurement of the elapsed time. Enzyme Unit (EU) was calculated using the equation $(t_o\text{-}t_c/t_c)$ where t_o and t_c are the times for pH change of the nonenzymatic and the enzymatic reactions, respectively.

Inhibition assay

The inhibitory effects of compounds **4a-4k** and AAZ on the hydratase activity of hCA I and hCA II isoenzymes were investigated. IC_{50} values were calculated for the compounds at different concentrations while maintaining a constant substrate concentration. The activities of enzymes in the medium without inhibitors were used as 100% activity. The activity% values of enzymes were calculated by measuring the hydratase activity in the presence of different concentrations of inhibitors. The IC_{50} value was calculated by utilizing graphs of activity%-[I] for each inhibitor [60–62]. Inhibition constants were calculated by the nonlinear least squares method using the Cheng-Prusoff equation [63–65].

Antioxidant activity

TAS activity

The total antioxidant status (TAS) is determined by a commercial kit that is manufactured by Rel Assay Diagnostics. According to this method, the potential antioxidant structures in the sample are reduced from the dark blue-green ABTS radical form to the colorless reduced ABTS form. The alteration of absorbance at 660 nm is related to the total antioxidant capacity of the sample. The assay was calibrated with the reference substance used as the stable standard antioxidant solution, which is the vitamin E analog called the Trolox equivalent. TAS measurement was performed according to the kit procedure. After calculating the difference between absorbance values, the equation given below is calculated according to Eq. 1 [66].

$$\begin{aligned} A_2 - A_1 &= \Delta\text{Abs of standart or sample or } H_2O \\ \text{Results} &= [\Delta\text{Abs } H_2O - \Delta\text{Abs Sample}]/ \\ &= [\Delta\text{Abs } H_2O - \Delta\text{Abs Standart}] \end{aligned} \quad (1)$$

Cytotoxicity assay

Cell culture

L929, the fibroblast cell line is purchased from American Type Culture Collection and grown in Dulbecco's modified Eagle's medium (DMEM; Gibco, Thermo Fisher Scientific), supplemented with 10% fetal bovine serum (FBS; Sigma Aldrich), 1% L-glutamine (Sigma-Aldrich), and 1% penicillin/streptomycin (Sigma-Aldrich). The cultured cells were incubated at 37 °C in a humidified atmosphere containing 5% CO_2. All newly synthesized compounds were dissolved in DMSO, and stock solutions were diluted with DMEM as the final concentration of DMSO did not exceed 0.5%.

Cell viability assay

The effect of the compounds between **4a-4k** on the viability of L929 cell line was analyzed by MTT assay. The cells were seeded at a density of 1×10^4 cells/well and treated with 100 µM concentrations for each and incubated for 48 h. Untreated cells were used as control. Following incubation, the cells were treated with 20 µL of MTT solution (5 mg/mL in PBS, Sigma) and incubated at 37 °C for 3 h to let the metabolically active cells reduce MTT dye into formazan crystals. The formazan crystals were dissolved in DMSO

(Sigma). The reduction of MTT was quantified by measuring the absorbance at 540 nm with a microplate reader (Thermo, Germany). Datas were represented as mean ± standard deviation (± SD).

Molecular docking

All stages of molecular docking studies were carried out using Schrödinger software Maestro 12.8 version. 3D structures of target proteins hCA I (PDB ID: 3W6H, Resolution: 2.96 Å) [67] and hCA II (PDB ID: 4G0C, Resolution: 2.00 Å) [68] were obtained from the protein data bank (PDB) https://www.rcsb.org/. Water and other heteroatoms other than Zn^{2+} were removed and target proteins were prepared with the 'Protein Preparation Wizard' default settings. The 3D minimizing structures of the compounds **4a-4k** were prepared with the 'LigPrep' module at pH:7 ± 2. The active site coordinates file for both target proteins hCA I (x: 33.6, y: −1.33, z: 9.01) and hCA II (x: −4.98, y: 3.81, z: 14.7) were created as 20*20*20 $Å^3$ with the 'Receptor Grid Generation' module based on the cocrystal ligand acetazolamide. To validate the molecular docking work, re-docking was performed with Glide SP and the cocrystal ligand acetazolamide. Then, molecular docking of all compounds with Glide SP ligand was performed [69].

Acknowledgements The authors thank Ankara University-Scientific Research Unit for supplying the Schrödinger software purchased under grant project number BAP-21B0237004.

Compliance with ethical standards

Conflict of interest The authors declare no competing interests.

Publisher's note Springer Nature remains neutral with regard to jurisdictional claims in published maps and institutional affiliations.

References

1. Townsend LB, Wise DS. The synthesis and chemistry of certain anthelmintic benzimidazoles. Parasitol Today. 1990;6:107–12. https://doi.org/10.1016/0169-4758(90)90226-T.
2. Pabba C, Wang HJ, Mulligan SR, Chen ZJ, Stark TM, Gregg BT. Microwave-assisted synthesis of 1-aryl-1H-indazoles via one-pot two-step Cu-catalyzed intramolecular N-arylation of arylhydrazones. Tetrahedron Lett. 2005;46:7553–7. https://doi.org/10.1016/j.tetlet.2005.08.143.
3. Veerakumari L, Munuswamy N. In vitro effect of some anthelmintics on lactate dehydrogenase activity of Cotylophoron cotylophorum (Digenea: Paramphistomidae). Vet Parasitol. 2000;91:129–40. https://doi.org/10.1016/S0304-4017(00)00258-2.
4. Merino G, Jonker JW, Wagenaar E, Pulido MM, Molina AJ, Alvarez AI. et al. Transport of anthelmintic benzimidazole drugs by breast cancer resistance protein (BCRP/ABCG2). Drug Metab Dispos. 2005;33:614–8. https://doi.org/10.1124/dmd.104.003319.
5. Acar Çevik U, Sağlık BN, Osmaniye D, Levent S, Kaya Çavuşoğlu B, Karaduman AB. et al. Synthesis, anticancer evaluation and molecular docking studies of new benzimidazole-1, 3, 4-oxadiazole derivatives as human topoisomerase types I poison. J Enzyme Inhib. Med. Chem. 2020;35:1657–1673. https://doi.org/10.1080/14756366.2020.1806831.
6. Torres-Gómez H, Hernández-Núñez E, León-Rivera I, Guerrero-Alvarez J, Cedillo-Rivera R, Moo-Puc R. et al. Design, synthesis and in vitro antiprotozoal activity of benzimidazole-pentamidine hybrids. Bioorg Med Chem Lett. 2008;18:3147–51. https://doi.org/10.1016/j.bmcl.2008.05.009.
7. Iemura R, Kawashima T, Fukuda T, Ito K, Tsukamoto G. Synthesis of 2-(4-substituted-1-piperazinyl) benzimidazoles as H1-antihistaminic agents. J Med Chem. 1986;29:1178–83.
8. Kühler TC, Swanson M, Shcherbuchin V, Larsson H, Mellgård B, Sjöström JE. Structure− activity relationship of 2-[[(2-Pyridyl) methyl] thio]-1 H-benzimidazoles as anti helicobacter pylori agents in vitro and evaluation of their in vivo efficacy. J Med Chem. 1998;41:1777–88. https://doi.org/10.1021/jm970165r.
9. Horn J. The proton-pump inhibitors: similarities and differences. Clin Ther. 2000;22:266–80. https://doi.org/10.1016/S0149-2918(00)80032-6.
10. Vausselin T, Séron K, Lavie M, Mesalam AA, Lemasson M, Belouzard S. et al. Identification of a new benzimidazole derivative as an antiviral against hepatitis C virus. J Virol. 2016;90:8422–34. https://doi.org/10.1128/JVI.00404-16.
11. Okombo J, Brunschwig C, Singh K, Dziwornu GA, Barnard L, Njoroge M. et al. Antimalarial pyrido [1, 2-a] benzimidazole derivatives with Mannich base side chains: synthesis, pharmacological evaluation, and reactive metabolite trapping studies. ACS Infect Dis. 2019;5:372–84. https://doi.org/10.1021/acsinfecdis.8b00279.
12. Pan T, He X, Chen B, Chen H, Geng G, Luo H. et al. Development of benzimidazole derivatives to inhibit HIV-1 replication through protecting APOBEC3G protein. Eur J Med Chem. 2015;95:500–13. https://doi.org/10.1016/j.ejmech.2015.03.050.
13. Arnaiz DO, Griedel B, Sakata S, Dallas JL, Whitlow M, Trinh L. et al. Design, synthesis, and in vitro biological activity of benzimidazole based factor Xa inhibitors. Bioorg Med Chem Lett. 2000;10:963–6. https://doi.org/10.1016/S0960-894X(00)00139-6.
14. Clapp LB. Comp Het Chem. 6, ed. KT Potts, Pergamon Press: Oxford, 1984:365.
15. Paton RM. Comp Het Chem. 6, KT Potts, Pergamon Press: Oxford, 1984:393.
16. Hills J. Comp Het Chem. 6, KT Potts, Pergamon Press: Oxford, 1984:393.
17. Boström J, Hogner A, Llinàs A, Wellner E, Plowright AT. Oxadiazoles in medicinal chemistry. J Med Chem. 2012;55:1817–30. https://doi.org/10.1021/jm2013248.
18. Siwach A, Verma PK. Therapeutic potential of oxadiazole or furadiazole containing compounds. BMC Chem. 2020;14:1–40. https://doi.org/10.1186/s13065-020-00721-2.
19. Mishra P, Rajak H, Mehta A. Synthesis of Schiff bases of 2-amino-5-aryl-1, 3, 4-oxadiazoles and their evaluation for antimicrobial activities. J Gen Appl Microbiol. 2005;51:133–41. https://doi.org/10.2323/jgam.51.133.
20. Ahsan MJ, Samy JG, Khalilullah H, Nomani MS, Saraswat P, Gaur R. et al. Molecular properties prediction and synthesis of novel 1, 3, 4-oxadiazole analogues as potent antimicrobial and antitubercular agents. Bioorg Med Chem Lett. 2011;21:7246–50. https://doi.org/10.1016/j.bmcl.2011.10.057.
21. Rajak H, Singour P, Kharya MD, Mishra P. A novel series of 2, 5-disubstituted 1, 3, 4-oxadiazoles: synthesis and SAR study for their

anticonvulsant activity. Chem Biol Drug Des. 2011;77:152–8. https://doi.org/10.1111/j.1747-0285.2010.01066.x.
22. Srinivas M, Satyaveni S, Ram B. Design and synthesis of 1, 3, 4-oxadiazole incorporated indole derivatives as anticancer agents. J Pharm Res. 2018;12:758–63.
23. Vinayak A, Sudha M, Lalita KS. Design, synthesis and characterization of novel amine derivatives of 5-[5-(chloromethyl)-1,3, 4-oxadiazol-2-yl]-2-(4-fluorophenyl)-pyridine as a new class of anticancer agents. Dhaka Univ J Pharm Sci. 2017;16:11–19. https://doi.org/10.3329/dujps.v16i1.33377.
24. Martínez R, Zamudio GJN, Pretelin-Castillo G, Torres-Ochoa RO, Medina-Franco JL, Pinzón CIE. et al. Synthesis andantitubercular activity of new N-[5-(4-chlorophenyl)-1, 3, 4-oxadiazol-2-yl]-(nitroheteroaryl) carboxamides. Heterocycl Commun.2019;25:52–59. https://doi.org/10.1515/hc-2019-0007.
25. Pattan SR, Rabara PA, Pattan JS, Bukitagar AA, Wakale VS, Musmade DS. Synthesis and evaluation of some novel substituted 1, 3, 4-oxadiazole and pyrazole derivatives for antitubercular activity. Indian J Chem. 2009;2009:1453–6.
26. Somani RR, Agrawal AG, Kalantri PP, Gavarkar PS, Clercq ED. Investigation of 1, 3, 4-oxadiazole scaffold as potentially active compounds. Int J Drug Design Disc. 2011;2:353–60.
27. Malhotra M, Rawal RK, Malhotra D, Dhingra R, Deep A, Sharma PC. Synthesis, characterization and pharmacological evaluation of (Z)-2-(5-(biphenyl-4-yl)-3-(1-(imino) ethyl)-2, 3-dihydro-1, 3, 4-oxadiazol-2-yl) phenol derivatives as potent antimicrobial and antioxidant agents. Arab J Chem. 2017;10:S1022–31. https://doi.org/10.1016/j.arabjc.2013.01.005.
28. Biju CR, Ilango K, Prathap M, Rekha K. Design and microwave-assisted synthesis of 1,3,4-oxadiazole derivatives for analgesie and anti-inflammatory activity. J Young- Pharm. 2012;4:33–37. https://doi.org/10.4103/0975-1483.93576.
29. Supuran CT, Scozzafava A. Carbonic anhydrases as targets for medicinal chemistry. Bioorg Med Chem. 2007;15:4336–50. https://doi.org/10.1016/j.bmc.2007.04.020.
30. Scozzafava A, Passaponti M, Supuran CT, Gülçin İ. Carbonic anhydrase inhibitors: guaiacol and catechol derivatives effectively inhibit certain human carbonic anhydrase isoenzymes (hCA I, II, IX and XII). J Enzym Inhib Med Chem. 2015;30:586–91. https://doi.org/10.3109/14756366.2014.956310.
31. Kumar R, Vats L, Bua S, Supuran CT, Sharma PK. Design and synthesis of novel benzenesulfonamide containing 1,2,3-triazoles as potent human carbonic anhydrase isoforms I, II, IV and IX inhibitors. Eur J Med Chem. 2018;155:545–51. https://doi.org/10.1016/j.ejmech.2018.06.021.
32. Waheed A, Sly WS. Carbonic anhydrase XII functions in health and disease. Gene . 2017;623:33–40. https://doi.org/10.1016/j.gene.2017.04.027.
33. Stadie WC, O'Brien H. The catalysis of the hydration of carbon dioxide and dehydration of carbonic acid by an enzyme isolated from red blood cells. J Biol Chem. 1933;103:521–9. https://doi.org/10.1016/S0021-9258(18)75831-6.
34. Scozzafava A, Kalın P, Supuran CT, Gülçin İ, Alwasel SH. The impact of hydroquinone on acetylcholine esterase and certain human carbonic anhydrase isoenzymes (hCA I, II, IX, and XII). J Enzym Inhib Med Chem. 2015;30:941–6. https://doi.org/10.3109/14756366.2014.999236.
35. Alterio V, Di Fiore A, D'Ambrosio K, Supuran CT, De, Simone G. Multiple binding modes of inhibitors to carbonic anhydrases: how to design specific drugs targeting 15 different isoforms? Chem Rev. 2012;112:4421–68. https://doi.org/10.1021/cr200176r
36. Supuran CT. Carbonic anhydrases: Novel therapeutic applications for inhibitors and activators. Nat Rev Drug Disco. 2008;7:168–81. https://doi.org/10.1038/nrd2467.
37. Supuran CT. Structure and function of carbonic anhydrases. Biochem J. 2016;473:2023–32. https://doi.org/10.1042/BCJ20160115.
38. Supuran CT. Carbonic anhydrases and metabolism. Metabolites. 2018;8:25. https://doi.org/10.3390/metabo8020025.
39. Thiry A, Dogne JM, Supuran CT, Masereel B. Carbonic anhydrase inhibitors as anticonvulsant agents. Curr Top Med Chem 2007. 2007;7:855–64. https://doi.org/10.2174/156802607780636726.
40. Supuran CT. How many carbonic anhydrase inhibition mechanisms exist?. J Enzym Inhib Med Chem. 2016;31:345–60. https://doi.org/10.3109/14756366.2015.1122001.
41. Lock FE, McDonald PC, Lou Y, Serrano I, Chafe SC, Ostlund C, et al. Targeting carbonic anhydrase IX depletes breast cancer stem cells within the hypoxic niche. Oncogene. 2013;32:5210–9.
42. Bayram E, Senturk M, Kufrevioglu OI, Supuran CT. In vitro inhibition of salicylic acid derivatives on human cytosolic carbonic anhydrase isozymes I and II. Bioorg Med Chem. 2008;16:9101–5. https://doi.org/10.1016/j.bmc.2008.09.028.
43. Bozdag M, Pinard M, Carta F, Masini E, Scozzafava A, McKenna R. et al. A class of 4-sulfamoylphenyl-ω-aminoalkyl ethers with effective carbonic anhydrase inhibitory action and antiglaucoma effects. J Med Chem. 2014;57:9673–86. https://doi.org/10.1021/jm501497m.
44. Chegaev K, Lazzarato L, Tamboli Y, Boschi D, Blangetti M, Scozzafava A. et al. Furazan and furoxan sulfonamides are strong α-carbonic anhydrase inhibitors and potential antiglaucoma agents. Bioorg Med Chem. 2014;22:3913–21. https://doi.org/10.1016/j.bmc.2014.06.016.
45. De Luca L, Ferro S, Damiano FM, Supuran CT, Vullo D, Chimirri A. et al. Structure-based screening for the discovery of new carbonic anhydrase VII inhibitors. Eur J Med Chem. 2014;71:105–11. https://doi.org/10.1016/j.ejmech.2013.10.071.
46. Bruno E, Buemi MR, De Luca L, Ferro S, Monforte AM, Supuran CT. et al. In vivo evaluation of selective carbonic anhydrase inhibitors as potential anticonvulsant agents. Chem Med Chem. 2016;11:1812–8. https://doi.org/10.1002/cmdc.201500596.
47. Scozzafava A, Menabuoni L, Mincione F, Supuran CT. Carbonic anhydrase inhibitors. A general approach for the preparation of water-soluble sulfonamides incorporating polyamino− polycarboxylate tails and of their metal complexes possessing long-lasting, topical intraocular pressure-lowering properties. J Med Chem. 2002;45:1466–76. https://doi.org/10.1021/jm0108202.
48. Chinchilli KK, Angeli A, Thacker PS, Korra LN, Biswas R, Arifuddin M. et al. Design, synthesis, and biological evaluation of 1,2,3-Triazole-linked triazino [5,6-b] indole-benzene sulfonamide Conjugates as Potent Carbonic Anhydrase I, II, IX, and XIII Inhibitors. Metabolites. 2020;10:200. https://doi.org/10.3390/metabo10050200.
49. Kumar A, Siwach K, Rom T, Kumar R, Angeli A, Paul AK. et al. Tail-approach based design and synthesis of Arylthiazolylhydrazono-1,2,3-triazoles incorporating sulfanilamide and metanilamide as human carbonic anhydrase I, II, IV and IX inhibitors. Bioorg Chem. 2022;123:105764. https://doi.org/10.1016/j.bioorg.2022.105764.
50. Rafiq K, Ur Rehman N, Halim SA, Khan M, Khan A, Al-Harrasi A. Design, synthesis and molecular docking study of novel 3-phenyl-β-alanine-based oxadiazole analogues as potent carbonic anhydrase II inhibitors. Molecules. 2022;27:816. https://doi.org/10.3390/molecules27030816.
51. Saadiq M, Uddin G, Latif A, Ali M, Akbar N, Ammara, et al. Synthesis, bioactivity assessment, and molecular docking of non-sulfonamide benzimidazole-derived N-acylhydrazone scaffolds as carbonic anhydrase-II inhibitors. ACS Omega. 2021;7:705–15. https://doi.org/10.1021/acsomega.1c05362.
52. Gondru R, Li Y, Banothu J. Coumarin–benzimidazole hybrids: A review of developments in medicinal chemistry. Eur J Med Chem. 2022;227:113921. https://doi.org/10.1016/j.ejmech.2021.113921.

53. Alkhaldi AA, Al-Sanea MM, Nocentini A, Eldehna WM, Elsayed ZM, Bonardi A. et al. 3-Methylthiazolo [3,2-a] benzimidazole-benzenesulfonamide conjugates as novel carbonic anhydrase inhibitors endowed with anticancer activity: Design, synthesis, biological and molecular modeling studies. Eur J Med Chem. 2020;207:112745. https://doi.org/10.1016/j.ejmech.2020.112745.
54. Çevik UA, Celik I, Işık A, Pillai RR, Tallei TE, Yadav R. et al. Synthesis, molecular modeling, quantum mechanical calculations and ADME estimation studies of benzimidazole-oxadiazole derivatives as potent antifungal agents. J Mol Struct. 2022;1252:132095. https://doi.org/10.1016/j.molstruc.2021.132095.
55. Celik I, Erol M, Kuyucuklu G. Molecular modeling, density functional theory, ADME prediction and antimicrobial activity studies of 2-(substituted) oxazolo [4,5-b] pyridine derivatives. N. J Chem. 2021;45:11108–18. https://doi.org/10.1039/D1NJ00701G.
56. Işık A, Acar Çevik U, Karayel A, Celik I, Erçetin T, Koçak A. et al. Synthesis and molecular modelling of thiadizole based hydrazone derivatives as acetylcholinesterase and butyrylcholinesterase inhibitory activities. SAR QSAR Environ Res. 2022;33:1–22. https://doi.org/10.1080/1062936X.2022.2041723.
57. Arslan O, Nalbantoglu B, Demir N, Ozdemir H, Kufrevioglu OI. A new method for the purification of carbonic anhydrase isozymes by affinity chromatography. Turk J Med Sci. 1996;26:163–6.
58. Demir N, Demir Y, Nadaroglu H. Carbonic anhydrase from bovine bone. Prep Biochem Biotechnol. 2001;31:33–47. https://doi.org/10.1081/PB-100103370.
59. Demir Y, Demir N, Yildirim S, Nadaroglu H, Karaosmanoglu M, Bakan E. The activities of carbonic anhydrase and alkaline phosphatase in ancient human bones. Purification and characterization of outer peripheral, cytosolic, inner peripheral, and integral CA. Prep Biochem Biotechnol. 2001;31:291–304. https://doi.org/10.1081/PB-100104910.
60. Wilbur KM, Anderson NG. Electrometric and colorimetric determination of carbonic anhydrase. J Biol Chem. 1948;176:147–54. https://doi.org/10.1016/S0021-9258(18)51011-5.
61. Rickli EE, Ghazanfar SA, Gibbons BH, Edsall JT. Carbonic anhydrases from human erythrocytes. Preparation and properties of two enzymes. J Biol Chem. 1964;239:1065–78.
62. Altintop MD, Ozdemir A, Kucukoglu K, Turan-Zitouni G, Nadaroglu H, Kaplancikli Z. Synthesis and evaluation of new thiadiazole derivatives as potential inhibitors of human carbonic anhydrase isozymes (hCA-I and hCA-II). J Enzym Inhib Med Chem. 2015;30:32–37. https://doi.org/10.3109/14756366.2013.873038.
63. Borras J, Scozzafava A, Menabuoni L, Mincione F, Briganti F, Mincione G. et al. Carbonic anhydrase inhibitors: synthesis of water-soluble, topically effective intraocular pressure lowering aromatic/heterocyclic sulfonamides containing 8-quinoline-sulfonyl moieties: is the tail more important than the ring?. Bioorg Med Chem. 1999;7:2397–406. https://doi.org/10.1021/jm9900523.
64. Akocak S, Lolak N, Vullo D, Durgun M, Supuran CT. Synthesis and biological evaluation of histamine Schiff bases as carbonic anhydrase I, II, IV, VII, and IX activators. J Enzym Inhib Med Chem. 2017;32:1305–12. https://doi.org/10.1080/14756366.2017.1386660.
65. Küçükbay H, Buğday N, Küçükbay FZ, Berrino E, Bartolucci G, Del Prete S. et al. Synthesis and carbonic anhydrase inhibitory properties of novel 4-(2-aminoethyl) benzenesulfonamide-dipeptide conjugates. Bioorg Chem. 2019;83:414–23. https://doi.org/10.1016/j.bioorg.2018.11.003.
66. Erel O. A novel automated direct measurement method for total antioxidant capacity using a new generation, more stable ABTS radical cation. Clin Biochem. 2004;3:277–85. https://doi.org/10.1016/j.clinbiochem.2003.11.015.
67. Takaoka Y, Kioi Y, Morito A, Otani J, Arita K, Ashihara E. et al. Quantitative comparison of protein dynamics in live cells and in vitro by in-cell 19 F-NMR. Chem Commun. 2013;49:2801–3. https://doi.org/10.1039/C3CC39205H.
68. Fisher SZ, Aggarwal M, Kovalevsky AY, Silverman DN, McKenna R. Neutron diffraction of acetazolamide-bound human carbonic anhydrase II reveals atomic details of drug binding. J Am Chem Soc. 2012;134:14726–9. https://doi.org/10.1021/ja3068098.
69. Friesner RA, Murphy RB, Repasky MP, Frye LL, Greenwood JR, Halgren TA. et al. Extra precision glide: Docking and scoring incorporating a model of hydrophobic enclosure for protein−ligand complexes. J Med Chem. 2006;49:6177–96. https://doi.org/10.1021/jm051256o.